

Dynamic Modeling Possibilities of Embedded Rail Structures

Zoltán Major^{1,2}, Attila Németh^{1,2}, Vivien Jóvér^{1,2}, Nándor Liegner³, Szabolcs Fischer^{1,2,*}

¹ Széchenyi István University, Central Campus Győr
Egyetem tér 1, H-9026 Győr, Hungary
{majorz,nemeth.attila,jover.vivien,fischersz}@sze.hu

² Széchenyi István University, Vehicle Industry Research Center
Egyetem tér 1, H-9026 Győr, Hungary

³Department of Highway and Railway Engineering, Budapest University of
Technology and Economics
Műgyetem rkp. 3, H-1111 Budapest, Hungary
liegner.nandor@emk.bme.hu

*Corresponding author e-mail: fischersz@sze.hu

Abstract: In Hungarian design practice, the Zimmermann-Eisenmann quasi-static design method is employed to dimension track structures with embedded rails. This method determines the mean values of deformations and stresses using an infinitely long elastically embedded beam as the static frame. After establishing these mean values, the effects of track condition and speed are considered through Eisenmann multiplication, enabling the definition of design values. Conversely, international practices include methods that calculate deformations and stresses based on dynamic models incorporating viscoelastic embedding, directly accounting for speed but not dynamic effects due to track characteristics. This paper presents a solution to the dynamic problem, extending it to studying rotating frames beyond the commonly considered uniaxial solution. Each factor's effect is separately analyzed for track structures with embedded rail tracks, leading to a recommendation for the value of the "load multiplication factor".

Keywords: embedded rail; ERS; dynamic modeling; parametric study

1 Introduction

Transportation efficiency plays a pivotal role in the sustainability and economic vitality of urban and specialized environments, where effective management systems are essential for optimizing resources and minimizing operational costs [1].

In particular, the optimization of transportation schedules, such as early garbage collection in metropolitan areas, directly impacts the overall efficiency and environmental footprint of city infrastructure, making it a critical area of study for modern urban planning [2]. As transportation systems become increasingly complex and integrated within urban infrastructure, the need for advanced modeling techniques to understand and improve these systems has never been more pressing.

Dynamic modeling of embedded rail structures is essential for understanding the behavior of rail systems within various track configurations. This research is critical for enhancing railway infrastructure's safety, efficiency, and durability by examining the dynamic responses to different loads and environmental conditions. This domain's primary areas of interest include vibration analysis, noise mitigation, system performance optimization, reliability assessment, life cycle costing, dynamic characteristic evaluation, flaw detection, and vehicle-track interaction.

In the following paragraphs, a detailed literature review is provided. The authors tried to collect as many related references as possible to introduce the topic's relevancy.

Numerous studies have delved into these areas extensively. For instance, Yeh *et al.* [3] used ANSYS software for finite element analysis to investigate vibration and noise in embedded rail systems. Additional research by Ling *et al.* [4] and Kuchak *et al.* [5, 6] explored the dynamic behavior of these systems, emphasizing their distinct dynamics compared to other slab tracks. Major [7] further contributed by discussing numerical modeling and optimization strategies for embedded rails, particularly for high-speed rail lines.

Kurhan and Fischer [8] showcased the use of elastic wave propagation in modeling dynamic rail deflection, providing valuable insights into the interaction between these waves and track material properties. Extending this analysis, Kurhan and Kurhan [9] modeled the dynamic behavior of rail systems under varying conditions using advanced computational methods. Kurhan and Leibuk [10] advanced the understanding of railway track dynamics by introducing a methodology for calculating the reduced mass of railway tracks, thereby enhancing the accuracy of dynamic models.

Shang *et al.* [11] developed a reliability-based life cycle costing model for embedded rails in level crossings, optimizing reliability, financial parameters, and maintenance strategies. Hao [12] offered insights into the performance of different ballastless rail structures, while Ézsiás *et al.* [13] examined ballast material behavior, focusing on mining and quarrying influences. Zhang *et al.* [14] presented a linearized model for flaw detection in rails, which is crucial for maintenance and safety.

The interaction between vehicles and tracks is another pivotal area of study. Kampczyk *et al.* [15] investigated how traction electricity consumption is affected by route geometry and vehicle characteristics. Dižo *et al.* [16] evaluated the running

properties of rail vehicles on real track models, stressing the importance of accurately replicating track conditions in simulations. Lei [17] added to this body of knowledge by developing a three-dimensional finite element model for high-speed railway track structures, while Gallou et al. [18] used finite element analysis to assess rail joint deflection behavior.

Gong et al. [19] modeled the interaction of out-of-round wheels with flexible tracks at rail welds using Euler-Bernoulli beams, which is vital for understanding wear and fatigue in rail components. Kou et al. [20] focused on rail wear and rolling contact fatigue, particularly in high-stress areas like frog rails, providing crucial insights for extending the service life of rail components and optimizing maintenance strategies.

Energy efficiency in rail systems has also garnered significant attention. Fischer and Szürke [21] discussed energy loss detection in electric railway vehicles, integrating energy efficiency considerations into rail system design and operation. Elmoghazy et al. [22] explored the dynamic response of viscoelastic sandwiched structures, emphasizing the importance of material properties in the overall behavior of rail systems. Köken [23, 24] made notable contributions to material characterization using artificial neural networks and soft computing techniques, which are valuable for designing and maintaining rail infrastructure in geologically complex regions.

In the context of education and sustainability, Barać et al. [25] highlighted the role of educational platforms in promoting clean production within mechanical engineering, which is relevant for the future of railway design and construction. Shabana et al. [26] proposed a multi-body system approach for finite element modeling of rail flexibility, while Xiao et al. [27] studied the initiation of rail corrugation under track vibration.

An et al. [28] analyzed the dynamic response of wheel-rail interaction at rail welds in high-speed railways, and Wang and Lei [29] investigated the causes and development of rail corrugation on metro tracks. Huo et al. [30] developed a rigid-flexible coupling dynamic model for bearing-wheel-rail systems under track irregularities. Lastly, Mazilu et al. [31] introduced a nonlinear track model with elastic layers and inertial components, enhancing the understanding of rail track behavior.

Despite substantial research efforts, a comprehensive understanding of the combined effects of track conditions and vehicle speed on dynamic behavior remains elusive. Current studies often concentrate on specific aspects such as vibration, noise, and reliability, employing methods like finite element analysis, multi-body dynamics, and reliability-based life cycle costing. However, these approaches frequently rely on quasi-static design methods or dynamic models that insufficiently address track irregularities and dynamic loads at varying speeds. There is a pressing need for an integrated dynamic model that encompasses track conditions, vehicle speed, and dynamic load amplification to improve the reliability and safety of embedded rail structures. Such a model would enable more accurate

predictions of deformations and stresses, informing better maintenance practices and optimization strategies.

In Hungarian design practice, the Zimmermann-Eisenmann quasi-static design method is used to calculate mean deformations and stresses, incorporating track conditions and speed to establish design values. International methodologies incorporate viscoelastic embedding and speed effects but often lack a standardized "load-increasing factor" to reflect dynamic effects in design specifications adequately. Developing a comprehensive dynamic model that addresses these gaps would significantly enhance the reliability and safety of embedded rail structures.

This article presents a solution to the dynamic modeling challenge and examines the impact of various factors on track structures with embedded rails.

The structure of the current article is as follows: Section 2 deals with the materials and methods, Section 3 is about results, Section 4 is the discussion, and Section 5 contains conclusions.

2 Materials and Methods

2.1 Description of the Model

The deflection due to a moving load on a curved beam lying on a viscoelastic bed frame can be determined from Eq. (1).

$$E_s I_s \frac{\partial^4 w(x,t)}{\partial x^4} + m \frac{\partial^2 w(x,t)}{\partial t^2} + D \frac{\partial w(x,t)}{\partial t} + (U_{dyn} \cdot 10^6) \cdot w(x,t) = 0 \quad (1)$$

where:

- E_s : modulus of elasticity of the rail material [N/m²],
- I_s : the moment of inertia of the rail on the horizontal axis [m⁴],
- $E_s I_s$: the bending stiffness of the rail [Nm²],
- m : the specific mass of the track structure [kg/m],
- D : damping specific to the track structure [Ns/m],
- U_{dyn} : dynamic rail support stiffness specific to the track structure [N/mm/mm],
- $w(x,t)$: rail deflection [m].

The model of the dynamically loaded structure is shown in Figure 1.

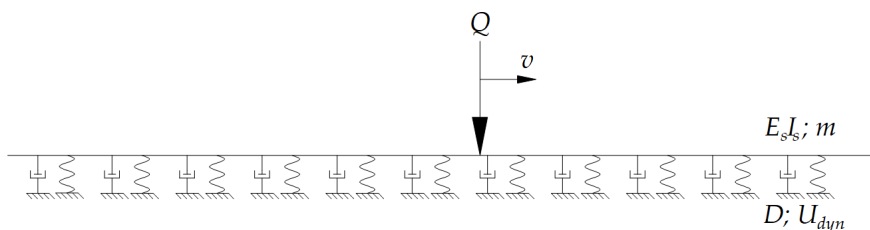


Figure 1

The model of the dynamically loaded structure

Fryba provided a computational method for the solution [32], which was also published by Rapp [33]. In the article, the authors present the solution according to the notation of Rapp [33]. The first step in the solution is to determine the stiffness length of the rail, which is similar to the Zimmermann derivation – see Eq. (2).

$$L = 4 \sqrt{\frac{E_s I_s}{U_{dyn}}} \quad (2)$$

where:

- L : the stiffness length [mm].

Similar to the Zimmermann derivation, the x coordinates (alongside the railway track) are transformed as a function of the stiffness length according to Eq. (3).

$$\xi = \frac{x}{L} \quad (3)$$

The dynamic characteristics are considered in the derivation using two auxiliary dimensionless quantities. The first is the ratio (α) of the vehicle speed (v) to the critical speed (v_{cr}) – see Eq. (4).

$$\alpha = \frac{v}{v_{cr}} \quad (4)$$

The other is the ratio (β) of the track-specific damping (D) to the critical damping (D_{cr}) – see Eq. (5).

$$\beta = \frac{D}{D_{cr}} \quad (5)$$

The calculation of the two factors and their impact on the results will be discussed in more detail later in this article.

Knowing these, the required deflection function can be obtained in Eqs. (6-7).

if, $x \geq 0$:

$$w(x, t) = \frac{Q}{2 \cdot L \cdot U_{dyn}} \cdot \left[\frac{2}{a_1 \cdot (A_1^2 + A_2^2)} \cdot e^{-a_0 \cdot \xi} \cdot (A_1 \cdot \cos(a_1 \cdot \xi) + A_2 \cdot \sin(a_1 \cdot \xi)) \right] \quad (6)$$

if, $x < 0$:

$$w(x, t) = \frac{Q}{2 \cdot L \cdot U_{dyn}} \cdot \left[\frac{2}{a_2 \cdot (A_3^2 + A_4^2)} \cdot e^{a_0 \cdot \xi} \cdot (A_3 \cdot \cos(a_2 \cdot \xi) + A_4 \cdot \sin(a_2 \cdot \xi)) \right] \quad (7)$$

The auxiliary quantities in the formula can be calculated using Eqs. (8-14).

$$a_0 = \sqrt{1 - \alpha^2} \quad (8)$$

$$a_1 = \sqrt{1 + \alpha^2 + 2 \cdot \alpha \cdot \beta \cdot \sqrt{\frac{1}{1 - \alpha^2}}} \quad (9)$$

$$a_2 = \sqrt{1 + \alpha^2 - 2 \cdot \alpha \cdot \beta \cdot \sqrt{\frac{1}{1 - \alpha^2}}} \quad (10)$$

$$A_1 = a_0 \cdot a_1 \quad (11)$$

$$A_2 = a_0^2 - 0.25 \cdot (a_1^2 - a_2^2) \quad (12)$$

$$A_3 = a_0 \cdot a_2 \quad (13)$$

$$A_4 = a_0^2 + 0.25 \cdot (a_1^2 - a_2^2) \quad (14)$$

2.2 Determination of Specific Mass and Dynamic Rail Stiffness

Determining an embedded rail track structure's specific mass is challenging on purely theoretical grounds. The vibrating mass includes the mass of the rail and part of the pouring material. The problem can be solved by finite element modeling. The model for calculating the static spring constant must first be constructed to fulfill this. The nominal under-pouring thickness for the structure is 31 mm. The parameters for the pouring material are summarized in Table 1. The rail profile/system used is 60E1. The vertical deflection of the 10 mm thick model is 0.906 mm. Based on the displacement obtained for a 1000-mm-long model, the static rail support stiffness value (U_{stat}) can be calculated based on Eq. (15).

$$U_{stat} = \frac{1000}{10} \cdot \frac{1}{0.906} = 110.38 \text{ N/mm/mm} \quad (15)$$

If this static spring constant is applied to calculate the first vertical natural frequency (f_0) of the structure with only the weight of the rail of 60.21 kg/m, Eq. (16) can be obtained.

$$f_0 = \frac{1}{2\pi} \cdot \sqrt{\frac{110.38 \cdot 10^6}{60.21}} = 215.48 \text{ Hz} \quad (16)$$

Table 1

Material properties used to determine the static rail support stiffness

Characteristic parameter	Value	Unit
E	2.20	N/mm ²
ν	0.49	-
ρ	1050	kg/m ³

If the vibration test is performed using the model parameters used for static modeling. The first vertical natural frequency of the structure is obtained by the program – see Eq. (17).

$$f_0 = 197.01 \text{ Hz} \quad (17)$$

In the model, the channel walls are rigidly supported to investigate only the vibrations of the track structure. The difference between the calculated and modeled values is since the program considered the mass of the pouring material involved in the vibration. If the mass is calculated back from the natural frequency coefficient, the result is 72.01 kg/m. Subtracting the mass of the rail gives the mass of the co-vibrating pouring material, which is 11.8 kg/m.

This method can be used to determine the specific mass of any embedded rail structure based on simple assumptions.

Based on practical experience, the dynamic rail support stiffness value is 1.4 to 1.6 times the static value. Accurate values can be determined by laboratory testing for each of the embedded rail track designs. Using its mean value, the dynamic rail supporting stiffness value for the structure under investigation is shown in Eq. (18).

$$U_{dyn} = 1.5 \cdot U_{stat} = 1.5 \cdot 110.38 = 165.57 \text{ N/mm/mm} \quad (18)$$

The dynamic rail supporting stiffness and the co-vibrating mass can be used to determine the natural frequency of the structure, which can be determined by laboratory tests. The first vertical natural frequency of the structure under investigation is calculated as Eq. (19).

$$f_0 = \frac{1}{2\pi} \cdot \sqrt{\frac{165.57 \cdot 10^6}{72.01}} = 241.33 \text{ Hz} \quad (19)$$

2.3 Determination of the Critical Speed

The relation used for calculating a track structure for an embedded rail system can be found in [34], where the following relation for the square of the critical speed is given in Eq. (20).

$$v_{cr}^2 = \frac{2}{m} \cdot \sqrt{(U_{dyn} \cdot 10^6) \cdot E_s \cdot I_s} \quad (20)$$

by settling the equation this to the critical speed gives the following relationship:

$$v_{cr} = \sqrt[4]{\frac{4 \cdot (U_{dyn} \cdot 10^6) \cdot E_s \cdot I_s}{m^2}} \quad (21)$$

2.4 Determination of Damping Properties

Sebastian Rapp [33] discusses the calculation of the critical damping of a beam on a viscoelastic ballast bed. According to [33], the critical damping can be determined by Eq. (22).

$$D_{cr} = 4 \cdot L \cdot \sqrt{(U_{dyn} \cdot 10^6)} \cdot m \quad (22)$$

2.5 Quantifying the Practical Value of the Factors α and β

The parameter α is the ratio of the vehicle speed to the critical speed. Based on previous modeling, the specific mass of the track structure can be approximated by the mass of the rail. Only this is considered for simplification in the critical speed analysis. The previous formula (Eq. (21)) can be rearranged as Eq. (23).

$$v_{cr} = \sqrt[4]{\frac{4 \cdot E_s \cdot I_s \cdot 10^6}{m^2}} \cdot \sqrt[4]{U_{dyn}} \quad (23)$$

The first term of the above multiplication only contains the characteristics of the track system. Translating the relationship into a system factor form gives Eq. (24).

$$v_{cr} = c_v \cdot \sqrt[4]{U_{dyn}} \quad (24)$$

The system factor values for the rail systems used in practice are given in Table 2. The values reported in Table 2 were determined based on Eq. 25.

$$c_v = \sqrt[4]{\frac{4 \cdot E_s \cdot I_s \cdot 10^6}{m^2}} \quad (25)$$

Table 2

The c_v system factor values, considering different rail profiles.

Rail profiles/systems	c_v
SA42	192.87
49E1	279.86
54E1	283.09
60E1	288.27
53Ri1	249.81
59Ri1	295.33
60Ri1	294.53
Ts52	164.89
35GPB	184.72

3 Results and Discussion

Based on the system factors, the value of the critical speed as a function of the dynamic rail supporting stiffness can be determined. The calculated values are summarized in Figure 2.

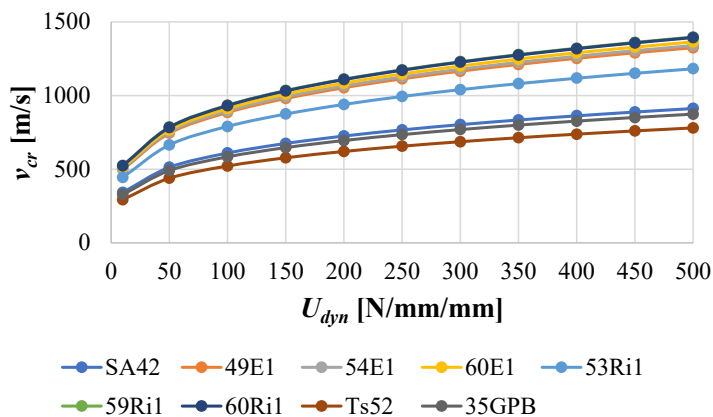


Figure 2

The value of the critical speed (v_{cr}) [m/s] considering different U_{dyn} values and different rail profiles.

Using these, someone can determine the maximum value of the parameter α that can be considered for Hungarian networks:

- in the case of the maximum permitted speed on the network of 44.4 m/s (160 km/h) for high-speed rail applications. The maximum values are summarized in Figure 3.
- in the case of the maximum permissible speed on the network of 19.4 m/s (70 km/h) for tramway applications. The maximum values are summarized in Figure 4.

It can be seen that considering the Hungarian conditions, the maximum value of the parameter α :

- $\alpha=0.09$ for high-speed rail applications/structures,
- $\alpha=0.07$ for high-speed rail applications.

If the value of the parameter is 0.00, the result is the same as the Zimmermann calculation.

The value of the parameter β can be determined by measurement, and in the current practical calculations, its value was set to 0.20. If the value of the parameter is 0.00, then the system is undamped.

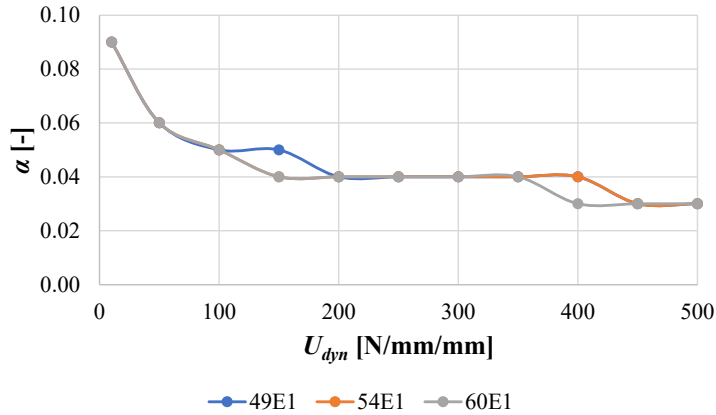


Figure 3

Maximum values of the parameter α at 160 km/h for high-speed rail applications/structures considering different U_{dyn} values and different rail profiles

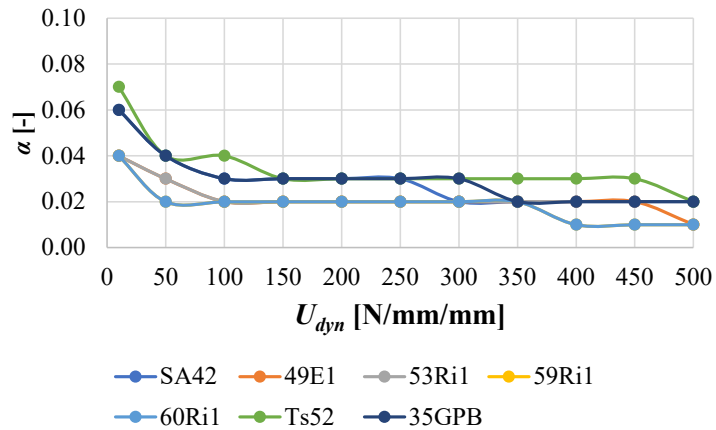


Figure 4

Maximum values of parameter α at 70 km/h for tram-track applications/structures considering different U_{dyn} values and different rail profiles

If someone takes $\alpha=0.10$ and $\beta=0.20$ as an approximation in favor of safety and plot the deflection action/effect diagram in a coordinate system and the one determined from the Zimmermann derivation ($\alpha=0.00$ and $\beta=0.00$), the authors find that the two action/effect diagrams practically run on each other, with only a slight difference in their values. (Figure 5) The main reason for this is that the speed of the vehicles is of the order of magnitude lower than the critical speed of the track structure.

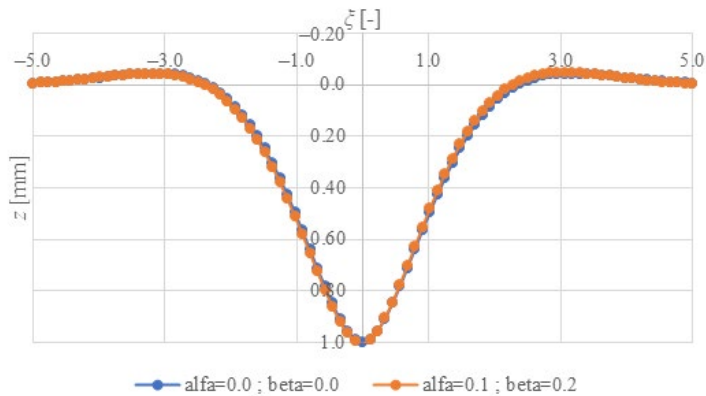


Figure 5

The calculated vertical deflection

Conclusions

This study provides a detailed dynamic analysis of track structures with embedded rail systems, emphasizing the practical significance and real-world application of various parameters. The results demonstrate that the Zimmermann-Eisenmann calculation method remains reliable and accurate for embedded rail track structures. This quasi-static approach effectively provides essential mean values for deformations and stresses, ensuring safe and efficient rail track design.

However, for other types of superstructures with different designs and dynamic characteristics, the suitability of this method should be carefully evaluated. The parameter analysis method proposed in this paper can serve as a valuable tool for assessing the applicability of the Zimmermann-Eisenmann method in these cases.

The importance of considering dynamic effects in track design is highlighted, especially for high-speed rail applications where vehicle speeds approach the track structure's critical speed. The study also underscores the potential for refining dynamic models to improve the accuracy and reliability of embedded rail track systems under various operating conditions.

In conclusion, while the Zimmermann-Eisenmann method is adequate for current embedded rail applications, further research and development of dynamic modeling techniques are necessary to ensure the safety and efficiency of future rail infrastructure. This study lays a solid foundation for such advancements and advocates for incorporating dynamic analysis into standard engineering practices for railway track design.

In our further research work, we would like to consider the associated speed-rail profile-stiffness/damping values for other countries as well. It can be considered a limitation of our present research because it only focuses on conditions in Hungary.

Nomenclature

- $a_0; a_1; A_1; a_2; A_2; A_3; A_4$: auxiliary quantities [-],
- c_v : the system factor for critical speed $[\frac{m}{s \cdot \sqrt[4]{N/mm/mm}}]$
- D : damping specific to the track structure [Ns/m],
- D_{cr} : critical damping of the track structure [Ns/m],
- E : elastic modulus of the pouring material [N/mm²],
- E_s : modulus of elasticity of the rail material [N/m²],
- $E_s I_s$: bending stiffness of the rail [Nm²],
- f_0 : natural frequency of the structure [Hz],
- I_s : the moment of inertia of the rail on the horizontal axis [m⁴],
- L : stiffness length [mm],
- m : specific mass of the track structure [kg/m],
- U_{dyn} : dynamic rail support stiffness specific to the track structure [N/mm/mm],
- U_{stat} : static rail support stiffness specific to the track structure [N/mm/mm],
- v : speed of the vehicle [m/s],
- v_{cr} : critical speed of the track structure [m/s],
- $w(x,t)$: rail deflection [mm],
- x : coordinates along the rail [m],
- z : vertical deflection [mm],
- α : ratio of the vehicle speed to the critical speed [-],
- β : ratio of the track-specific damping to the critical damping [-],
- ν : Poisson's ratio of the pouring material [-],
- ζ : ratio of the ordinates to the stiffness length [-],
- ρ : density of the pouring material [kg/m³].

Acknowledgement

This paper was prepared by the research team "SZE-RAIL". This research was supported by SIU Foundation's project 'Sustainable railways—Investigation of the energy efficiency of electric rail vehicles and their infrastructure'. The publishing of the paper did not receive financial support or financing of the APC.

References

- [1] Volkov, V., Taran, I., Volkova, T., Pavlenko, O., & Berezhnaja, N. (2020) Determining the efficient management system for a specialized transport enterprise. *Naukovyi Visnyk Natsionalnoho Hirnychoho Universytetu* (4) 185-191
- [1] Saukenova, I., Oliskevych, M., Taran, I., Toktamyssova, A., Aliakbarkyzy, D., & Pelo, R. (2022) Optimization of schedules for early garbage collection and disposal in the megapolis. *Eastern-European Journal of Enterprise Technologies*, 1(3(115)), 13-23

-
- [3] Yeh, F., Chang, X., & Sung, Y. (2017) Numerical and experimental study on vibration and noise of embedded rail system. *Journal of Applied Mathematics and Physics*, 5(9), 1629-1637
- [4] Ling, L., Han, J., Xiao, X., & Jin, X. (2015) Dynamic behavior of an embedded rail track coupled with a tram vehicle. *Journal of Vibration and Control*, 23(16), 2355-2372
- [5] Kuchak, A. J. T., Marinkovic, D., & Zehn, M. (2021) Parametric investigation of a rail damper design based on a lab-scaled model. *Journal of Vibration Engineering & Technologies*, 9(1), 51-60
- [6] Kuchak, A. J. T., Marinkovic, D., & Zehn, M. (2020) Finite element model updating—Case study of a rail damper. *Structural Engineering and Mechanics*, 73(1), 27-35
- [7] Major, Z. (2015) A method for the numerical modelling of embedded rails and determining parameters to be optimized. *Acta Technica Jaurinensis*, 9(1), 16-28
- [8] Kurhan, D., & Fischer, S. (2022) Modeling of the dynamic rail deflection using elastic wave propagation. *Journal of Applied and Computational Mechanics*, 8(1), 379-387
- [9] Kurhan, D., & Kurhan, M. (2019) Modeling of rail deflection using elastic wave propagation. *IOP Conference Series: Materials Science and Engineering*, 708, 012013
- [10] Kurhan, D., & Leibuk, Y. (2020) Research of the reduced mass of the railway track. *Acta Technica Jaurinensis*, 13(4), 324-341
- [11] Shang, Y., Boomen, M., Man, A., & Wolfert, A. (2019) Reliability-based life cycle costing analysis for embedded rails in level crossings. *Proceedings of the Institution of Mechanical Engineers, Part F: Journal of Rail and Rapid Transit*, 234(7), 821-833
- [12] Hao, N. (2023) Research on dynamic characteristics of the turnover system of rail belt conveyor. *Measurement Science and Technology*, 35(2), 025116
- [13] Ézsiás, L., Tompa, R., & Fischer, S. (2024) Investigation of the possible correlations between specific characteristics of crushed stone aggregates. *Spectrum of Mechanical Engineering and Operational Research*, 1(1), 10-26
- [14] Zhang, Z., Udpa, L., Udpa, S., Athavale, A., Utrata, D., Si, J., & Sun, Y. (1996) Linearized MFL model for embedded flaw detection in rails. In *Proceedings of the 19th International Conference on Nondestructive Testing* (pp. 553-560) New York, NY: Springer
- [15] Kampeczyk, A., Gamon, W., & Gawlak, K. (2023) Integration of traction electricity consumption determinants with route geometry and vehicle characteristics. *Energies*, 16(6), 2689

- [16] Dižo, J., Blatnický, M., Harušinec, J., & Suchánek, A. (2022) Assessment of dynamics of a rail vehicle in terms of running properties while moving on a real track model. *Symmetry*, 14(3), Article 536
- [17] Lei, X. (2001) Dynamic analysis of the track structure of a high-speed railway using finite elements. *Proceedings of the Institution of Mechanical Engineers, Part F: Journal of Rail and Rapid Transit*, 215(4), 301-309
- [18] Gallou, M., Frost, M., El-Hamalawi, A., & Hardwick, C. (2018) Assessing the deflection behaviour of mechanical and insulated rail joints using finite element analysis. *Proceedings of the Institution of Mechanical Engineers, Part F: Journal of Rail and Rapid Transit*, 232(9), 2290-2308
- [19] Gong, L., Chen, R., Wang, P., Xu, J., An, B., & Chen, J. (2020) Influence of out-of-round wheels on the vehicle–flexible track interaction at rail welds. *Proceedings of the Institution of Mechanical Engineers, Part F: Journal of Rail and Rapid Transit*, 235(3), 313-327
- [20] Kou, L., Sysyn, M., & Liu, J. (2024) Influence of crossing wear on rolling contact fatigue damage of frog rail. *Facta Universitatis, Series: Mechanical Engineering*, 22(1), 25-44
- [21] Fischer, S., & Szürke, S. K. (2023) Detection process of energy loss in electric railway vehicles. *Facta Universitatis, Series: Mechanical Engineering*, 21(1), 81-99
- [22] Elmoghazy, Y. H., Safaei, B., & Sahmani, S. (2023) Finite element analysis for dynamic response of viscoelastic sandwiched structures integrated with aluminum sheets. *Facta Universitatis, Series: Mechanical Engineering*, 21(4), 591-614
- [23] Köken, E. (2022) Estimation of deformation modulus of coals using artificial neural networks (ANN) *Acta Technica Jaurinensis*, 15(3), 125-129
- [24] Köken, E. (2024) Estimating uniaxial compressive strength of pyroclastic rocks using soft computing techniques. *Journal of Mining and Environment*, 15(3), 977-990
- [25] Barać, M., Vitković, N., Stanković, Z., Rajić, M., & Turudija, R. (2024) Description and utilization of an educational platform for clean production in mechanical engineering. *Spectrum of Mechanical Engineering and Operational Research*, 1(1), 145-158
- [26] Shabana, A., Chamorro, R., & Rathod, C. (2008) A multi-body system approach for finite-element modelling of rail flexibility in railroad vehicle applications. *Proceedings of the Institution of Mechanical Engineers, Part K: Journal of Multi-Body Dynamics*, 222(1), 1-15
- [27] Xiao, H., Song, Y., Wang, H., & Wu, S. (2018) Initiation and development of rail corrugation based on track vibration in metro systems. *Proceedings of*

- the Institution of Mechanical Engineers, Part F: Journal of Rail and Rapid Transit, 232(9), 2228-2243
- [28] An, B., Wang, P., Xiao, J., Xu, J., & Chen, R. (2017) Dynamic response of wheel-rail interaction at rail weld in high-speed railway. Shock and Vibration, 2017, 1-11
- [29] Wang, Z., & Lei, Z. (2020) Causes and development characteristics of corrugation on tangential track of metro. Journal of Vibroengineering, 22(7), 1814-1825
- [30] Huo, J., Wu, H., Zhu, D., Sun, W., Wang, L., & Dong, J. (2017) The rigid-flexible coupling dynamic model and response analysis of bearing-wheel-rail system under track irregularity. Proceedings of the Institution of Mechanical Engineers, Part C: Journal of Mechanical Engineering Science, 232(21), 3859-3880
- [31] Mazilu, T., Arsene, S., & Cruceanu, I. (2021) Track model with nonlinear elastic characteristic of the rubber rail pad. Materiale Plastice, 58(3), 84-98
- [32] Frýba L.: 'Vibration of solids and structures under moving loads', Noordhoff International Publishing, Groningen, 1972
- [33] Rapp, S. (2017) Model for identifying point instabilities on the track in conventional ballast construction. Stuttgart, Germany: Universität Stuttgart (in German)
- [34] Esveld, C. (2001) Modern Railway Track (2nd ed.) Zaltbommel, The Netherlands: MRT-Productions